Remote Sensing of Environment 139 (2013) 50–59

Contents lists available at ScienceDirect

Remote Sensing of Environment

journal homepage: www.elsevier.com/locate/rse

# Surface velocities and ice-front positions of eight major glaciers in the Southern Patagonian Ice Field, South America, from 2002 to 2011

Minami Muto, Masato Furuya *

Department of Natural History Sciences, Graduate School of Science, Hokkaido University, N10W8, Kita-ku, Sapporo 060-0810, Japan

ARTICLE INFO

*Article history:*
Received 14 December 2012
Received in revised form 28 July 2013
Accepted 30 July 2013
Available online xxxx

*Keywords:*
Glacier velocity
Southern Patagonia
Calving glacier
Synthetic aperture radar

ABSTRACT

The Patagonian Ice Fields are known to have undergone rapid retreat of frontal positions and significant thinning of its glaciers over the past decades. However, surface velocities have been measured at only a few of these glaciers. Thus, it remains uncertain if and to what extent the glacier dynamics has changed over time and contributed to ice loss in these ice fields. In this study, we examine the temporal evolution of flow velocities and ice-front positions at eight major glaciers in the Southern Patagonian Ice Field (SPI; Hielo Patagónico Sur) by using Advanced Synthetic Aperture Radar (ASAR) images from the Environmental Satellite (Envisat) launched in 2002 by the European Space Agency and Advanced Land Observation Satellite/Phased Array-type L-band Synthetic Aperture Radar (ALOS/PALSAR) data recorded from 2002 to 2011. The examined eight glaciers include Glaciar Jorge Montt, Occidental, Pio XI (or Brüggen), O'Higgins, Viedma, Upsala, Perito Moreno, and Grey. Not all the glaciers revealed significant changes in frontal positions and flow velocities in the study period. We detected significant temporal velocity changes at Glaciar Upsala, Jorge Montt, Occidental, and Pio XI. Among these four glaciers, Glaciars Upsala, Jorge Montt, and Occidental revealed significant acceleration and terminus retreat and were undergoing dynamic-thinning. The markedly different absolute velocities but equally large longitudinal near-terminus stretching at the three glaciers support a calving model based on crevasse-depth criteria, which predict a calving position where crevasse-depths are equal to ice thickness; crevasse-depths are controlled by the longitudinal stretching rate. Meanwhile, Glaciar Pio XI revealed complex spatial and temporal evolution in surface velocities without significant retreat, and its dynamics remains enigmatic.



## 1. Introduction

The Southern Patagonian Ice Field (SPI; Hielo Patagónico Sur) contains the largest temperate glaciers in southern hemisphere and covers approximately 13,000 km$^2$ area from approximately 48.5°S to 51.5°S (Aniya, Sato, Naruse, Skvarca, & Casassa, 1996; Fig. 1). The SPI consists of 48 outlet glaciers with an average altitude of 1355 m above sea level. All these outlet glaciers, except for two, are calving (Aniya et al., 1996). The ones on the western Chilean side mostly calve into fjords as tidewater calving glaciers, whereas those on the eastern Argentina side terminate into proglacial lakes (Aniya et al., 1996; Warren & Aniya, 1999). Their retreat in the frontal positions and rapid thinning toward the end of the 20th century has been reported, suggesting a significant contribution to global sea level increases (Aniya, Sato, Naruse, Skvarca, & Casassa, 1997; Rignot, Rivera, & Casassa, 2003). Moreover, Gravity Recovery And Climate Experiment (GRACE) observation data recorded since 2002 indicate a total mass loss rate from both the Northern Patagonian Ice Field and the SPI to be ranging from –23.0 ± 9.0 Gt a$^{-1}$ to –26.0 ± 6.0 Gt a$^{-1}$ (Chen, Wilson, Tapley, Blankenship, & Ivins, 2007; Ivins et al., 2011; Jacob, Wahr, Pfeffer, & Swenson, 2012). GRACE-based mass-loss estimates in the beginning of the 21st century are larger than the corresponding volume loss rate derived in the late 20th century (Rignot et al., 2003). The recently reported surface height change rates, based on a time series of digital elevation models (DEMs), are also consistent with GRACE-based estimates, which indicates an even more rapid drawdown over the past decade (Willis, Melkonian, Pritchard, & Rivera, 2012).

While near-surface temperature increases associated with global warming presumably contribute to ice loss due to melting, the accelerated ice losses reported on Greenland and Antarctica have been linked to changes in glacier dynamics as well (Pritchard, Arthern, Vaughan, & Edwards, 2009; Rignot & Kanagaratnam, 2006; van den Broeke et al., 2009). In particular, many polar glaciers that calve into the ocean have undergone significant acceleration, known as dynamic thinning, and have thus further contributed to ice loss. However, recent studies demonstrate spatial–temporal complexities of the outlet glacier velocities in Greenland (Bevan, Murray, Luckman, Hanna, & Huybrechts, 2012; Moon, Joughin, Smith, & Howat, 2012). In contrast to these large polar glaciers, no detailed glacier velocity maps are available for the Patagonian Ice Fields with the exception of those for certain accessible glaciers (Naruse, Skvarca, Kadota, & Koizumi, 1992; Naruse, Skvarca,

* Corresponding author. Tel.: +81 11 706 2759.
*E-mail address:* furuya@mail.sci.hokudai.ac.jp (M. Furuya).

0034-4257/$ – see front matter © 2013 Elsevier Inc. All rights reserved.
http://dx.doi.org/10.1016/j.rse.2013.07.034

Satow, Takeuchi, & Nishida, 1995; Rivera, Corripio, Bravo, & Cisternas, 2012; Stueffer, Rott, & Skvarca, 2007; Sugiyama et al., 2011). Satellite-derived velocity maps are also limited to Glaciars Perito Moreno (Ciappa, Pietranera, & Battazza, 2010; Michel & Rignot, 1999; Rott, Stuefer, Siegel, Skvarca, & Eckstaller, 1998) and Glaciar Upsala

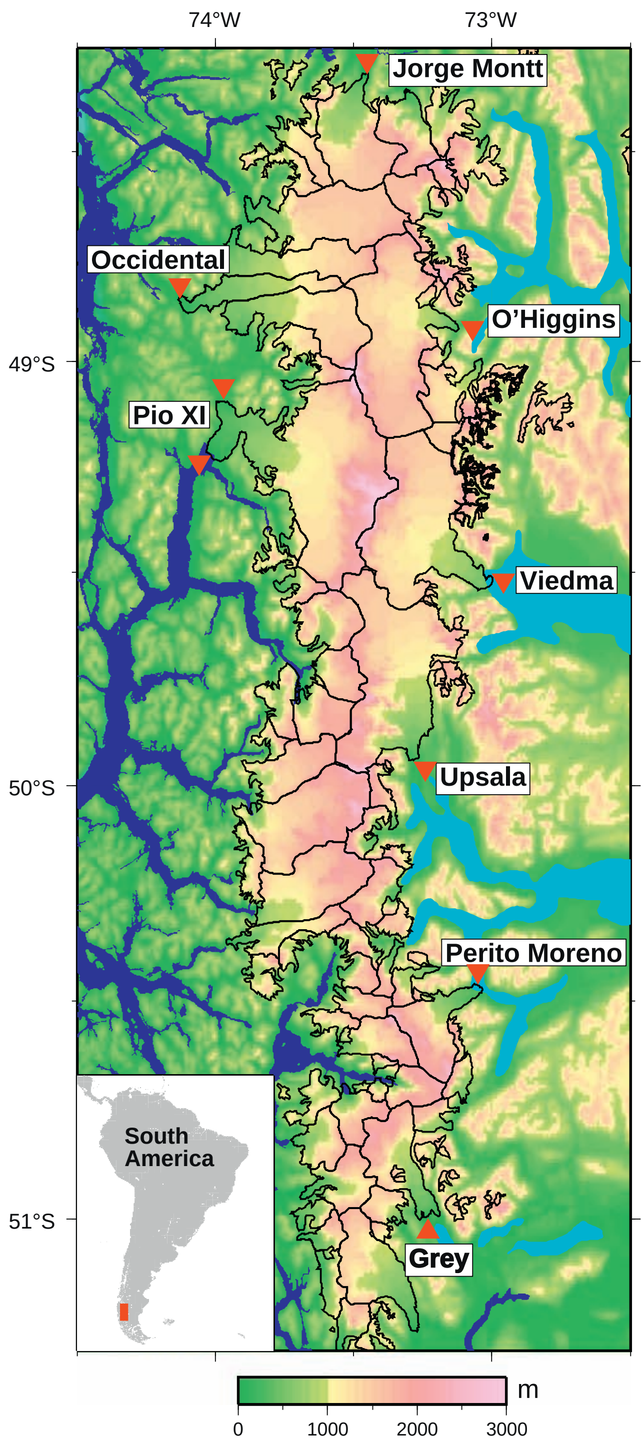


**Fig. 1.** Elevation map of the studied area and the glaciers in the South Patagonian Icefield; the elevation data set was obtained NASA's Shuttle Radar Topography Mission (SRTM). Red triangles represent the termini of the eight analyzed glaciers. Blue and light-blue indicate fjord and proglacial lakes, respectively. Glacier outlines were determined on the basis of the Global Land Ice Measurements from Space (GLIMS) dataset, which is available through the US National Snow and Ice Data Center (Dickmann, 2007; Delgado, 2009; Masiokas, 2009, 2010; Davies, 2012). (For interpretation of the references to color in this figure legend, the reader is referred to the web version of this article.)

(Floricioiu, Eineder, Rott, & Nagler, 2008; Floricioiu, Eineder, Rott, Yague-Martinez, & Nagler, 2009; Sakakibara, Sugiyama, Sawagaki, Marinsek, & Skvarca, 2013; Skvarca, Raup, & De Angelis, 2003). Thus, it remains uncertain if and to what extent dynamic thinning has affected the Patagonian Ice Fields. In this study, we show the spatial and temporal changes in flow velocities at eight major glaciers in the SPI by applying an offset tracking technique to the intensity images of the Environmental Satellite/Advanced Synthetic Aperture Radar (Envisat/ASAR) and Advanced Land Observation Satellite/Phased Array-type L-band Synthetic Aperture Radar (ALOS/PALSAR) data recorded from 2002 to 2011. In addition, we used the cloud-free characteristics of SAR imagery for examining the terminus changes in order to determine whether the ice acceleration is associated with calving episodes. The examined eight glaciers include Glaciars Upsala, Jorge Montt, Occidental, Pio XI (or Brüggen), O'Higgins, Viedma, Perito Moreno, and Grey (Fig. 1). We selected these glaciers not only because their sizes were sufficient to be imaged by the spatial resolution of presently available SAR data but also because they were more frequently imaged than others so that we could increase the temporal resolution, which allowed us to detect rapid changes in the ice dynamics.

As in the case of Greenland (Moon et al., 2012), we subsequently show that not all of the glaciers reveal ice acceleration and rapid terminus retreat. Submarine melting has been suggested as a principal triggering mechanism for the accelerated ice motion in Greenland, because the timing of the glacier's acceleration coincided with that of the ocean water warming near Greenland (Holland, Thomas, de Young, Ribergaard, & Lyberth, 2008; Rignot, Koppes, & Velicogna, 2010; Straneo et al., 2011). The rapid retreat and flow acceleration in the SPI, however, occur at both marine and fresh-water terminating glaciers, which suggests the presence of additional general processes independent of water salinity. While the physically based calving model remains elusive (Benn, Warren, & Mottram, 2007), we interpret the observed data sets on the basis of the calving model based on crevasse-depth criteria (Benn, Hulton, & Mottram, 2007; Benn, Warren, et al., 2007; Nick, van der Veen, Vieli, & Benn, 2010).

## 2. Data and analysis method

### 2.1. Satellite data

To generate glacier surface velocity maps, we processed the PALSAR images with a wavelength of 23.6 cm recorded from June 2007 to February 2011 from ALOS, which was launched in 2006 by the Japan Aerospace Exploration Agency (JAXA) (Table 1, Fig. 1). To extend the analysis period further back to 2003, we also used the C-band (wavelength of 5.6 cm) ASAR images from Envisat launched in 2002 by the European Space Agency (Table 1, Fig. 1), which often contains de-correlation problems; the advantage of the L-band over C-band was shown before (Rignot, 2008; Strozzi et al., 2008). On the basis of our observations of insignificant temporal velocity changes at Glaciar Perito Moreno (Supplementary material), the differences in penetration depths due to different wavelengths do not appear to affect the inferred velocities. This result is theoretically reasonable because the most significant changes in glacier-flow velocity profile are expected to occur near the glacier bed rather than near the surface (Cuffey & Paterson, 2010).

The off-nadir beam angle of PALSAR is 34.3°, which forms ~39° incident angle at the flat ground in the image center. There are two available imaging modes, fine beam single polarization (FBS, HH) and fine beam dual polarization (FBD; HH and HV). We used data from only HH polarization. The difference between FBS and FBD is the slant range (across track) resolution, which is ~4.7 m for the FBS mode and ~9.4 m for the FBD mode; the azimuth resolution is 3.1 m regardless of the mode. The FBD data are oversampled twice along the range axis. On